Small-scale effects of underwater bubble clouds on ocean reflectance: 3-D modeling results

Jacek Piskozub,[1,*] Dariusz Stramski,[2] Eric Terrill,[2] and W. Kendall Melville[2]

[1]*Institute of Oceanology, Polish Academy of Sciences, Powstancow Warszawy 55, 81-712 Sopot, Poland*
[2]*Marine Physical Laboratory, Scripps Institution of Oceanography, University of California, San Diego, La Jolla, CA 92093-0238, USA*
*piskozub@iopan.gda.pl

Abstract: We examined the effect of individual bubble clouds on remote-sensing reflectance of the ocean with a 3-D Monte Carlo model of radiative transfer. The concentrations and size distribution of bubbles were defined based on acoustical measurements of bubbles in the surface ocean. The light scattering properties of bubbles for various void fractions were calculated using Mie scattering theory. We show how the spatial pattern, magnitude, and spectral behavior of remote-sensing reflectance produced by modeled bubble clouds change due to variations in their geometric and optical properties as well as the background optical properties of the ambient water. We also determined that for realistic sizes of bubble clouds, a plane-parallel horizontally homogeneous geometry (1-D radiative transfer model) is inadequate for modeling water-leaving radiance above the cloud.

OCIS codes: (010.0280) Remote sensing; (010.4450) Ocean Optics; (010.4455) Oceanic propagation; (010.4458) Oceanic scattering; (010.5620) Radiative transfer.

References and links

1. X. Zhang, M. Lewis, and B. Johnson, "Influence of bubbles on scattering of light in the ocean," Appl. Opt. **37**(27), 6525–6536 (1998), http://www.opticsinfobase.org/ao/abstract.cfm?URI=ao-37-27-6525.
2. E. J. Terrill, W. K. Melville, and D. Stramski, "Bubble entrainment by breaking waves and their influence on optical scattering in the upper ocean," J. Geophys. Res. **106**(C8), 16815–16823 (2001).
3. D. Stramski, and J. Tęgowski, "Effects of intermittent entrainment of air bubbles by breaking wind waves on ocean reflectance and underwater light field," J. Geophys. Res. **106**(C12), 31345–31360 (2001).
4. P. Flatau, J. Piskozub, and J. R. Zaneveld, "Asymptotic light field in the presence of a bubble-layer," Opt. Express **5**(5), 120–124 (1999), http://www.opticsinfobase.org/oe/abstract.cfm?URI=oe-5-5-120.
5. J. Piskozub, T. Neumann, and L. Woźniak, "Ocean color remote sensing: choosing the correct depth weighting function," Opt. Express **16**(19), 14683–14688 (2008), http://www.opticsinfobase.org/oe/abstract.cfm?URI=oe-16-19-14683.
6. J. Piskozub, D. Stramski, E. Terrill, and W. K. Melville, "Influence of forward and multiple light scatter on the measurement of beam attenuation in highly scattering marine environments," Appl. Opt. **43**(24), 4723–4731 (2004), http://www.opticsinfobase.org/ao/abstract.cfm?URI=ao-43-24-4723.
7. D. McKee, J. Piskozub, and I. Brown, "Scattering error corrections for in situ absorption and attenuation measurements," Opt. Express **16**(24), 19480–19492 (2008), http://www.opticsinfobase.org/oe/abstract.cfm?URI=oe-16-24-19480.
8. R. M. Pope, and E. S. Fry, "Absorption spectrum (380-700 nm) of pure water. II. Integrating cavity measurements," Appl. Opt. **36**(33), 8710–8723 (1997), http://www.opticsinfobase.org/ao/abstract.cfm?URI=ao-36-33-8710.
9. R. C. Smith, and K. S. Baker, "Optical properties of the clearest natural waters (200–800 nm)," Appl. Opt. **20**(2), 177–184 (1981), http://www.opticsinfobase.org/ao/abstract.cfm?URI=ao-20-2-177.
10. A. Morel, "Light and marine photosynthesis: a spectral model with geochemical and climatological implications," Prog. Oceanogr. **26**(3), 263–306 (1991).
11. C. D. Mobley, B. Gentili, H. R. Gordon, Z. Jin, G. W. Kattawar, A. Morel, P. Reinersman, K. Stamnes, and R. H. Stavn, "Comparison of numerical models for computing underwater light fields," Appl. Opt. **32**(36), 7484–7504 (1993), http://www.opticsinfobase.org/ao/abstract.cfm?URI=ao-32-36-7484.

1. Introduction

The optical scattering within the near-surface layer of the ocean can be largely determined by air bubbles entrained by surface wave breaking [1,2]. However, bubble effects on the underwater light field and water-leaving light are complex and poorly understood. A previous study that utilized a 1-D radiative transfer model with plane-parallel geometry provided preliminary findings and indicated a need for a three-dimensional approach [3]. Whereas current satellite ocean color sensors have a spatial resolution of the order of 0.1 - 1 km, airborne sensors often provide measurements with a higher resolution, comparable to the spatial extent of individual bubble clouds of the order of several to tens of meters and space-based sensors may soon provide similar spatial resolution. Even for the current satellite sensors, sub-pixel variability due to bubble clouds may influence the measurement of pixel-average water-leaving radiance. The primary objective of this paper is to use 3-D Monte Carlo simulations of radiative transfer to provide preliminary insights into the variability of remote-sensing reflectance (RSR) just above the sea surface over "idealized" three-dimensional individual bubble clouds present in the near-surface ocean due to wave breaking.

2. Modeling

Modeling was performed with a 3-D Monte Carlo code previously used for both in-water light field studies [4,5] and optical instrumentation error testing [6,7]. Bubble size distributions used in the modeling had been derived from data collected during the HyCODE 2000 experiment as the averages for six void fraction ranges: 10^{-9}-10^{-8}, 10^{-8}-10^{-7}, 10^{-7}-10^{-6}, 10^{-6}-10^{-5}, 10^{-5}-10^{-4} and 10^{-4}-10^{-3} [6]. We used them to calculate bubble scattering phase functions from Mie scattering theory (the functions for 550 nm were assumed to hold at other wavelengths considered in this study [6]). In the modeling, we also used the following inherent optical properties (IOPs) of sea water: Pope and Fry [8] data for pure sea water absorption and Smith and Baker [9] for scattering (and absorption below 340 nm), Morel [10] for chlorophyll-based model of IOPs, Petzold phase function [6] for non-bubble particulate scattering and Rayleigh phase function for pure water. Inelastic processes were not considered.

In the first set of simulations, we used a model of the bubble cloud of 20 hemispherical concentric bubble layers (the underwater parts of spheres with the center at the horizontal sea surface). The values of scattering coefficient by bubbles b_{bub} increase from 0.0001 m^{-1} for the outermost layer to 20 m^{-1} for the inner core and are considered wavelength independent (Fig. 1). The inner core had a 1.5 m radius while the outermost radius was 15 m. The modeled cloud was placed in a 50 m x 50 m model box of unlimited depth. The results for the hemispherical model are presented in Figs. 2a and 2b. In the second set of simulations (results in Figs. 3-5), the bubble clouds were vertical cylinders bounded by the sea surface and an underwater horizontal plane (either at the depth of 2 m or a variable one). The flat bottom of the cloud together with varying radius, are meant to make it possible to compare the results with 1-D radiative transfer modeling where horizontal layers are usually used.

The upwelling (nadir) water-leaving radiance (L_w) values derived from the modeling results correspond to a 7 deg acceptance angle in air. Remote-sensing reflectance (RSR) was calculated as a ratio of L_w to downwelling irradiance E_d incident upon a flat surface. In each run, E_d was represented by two hundred million (2×10^8) virtual "photons" (with 30 deg sun zenith angle and 30% of diffuse radiation). The grid for calculating the water-leaving radiance was 35 by 35 elements, representing an ocean surface area of either 50 m by 50 m or 15 m by 15 m (depending on the size of the modeled bubble cloud). The downwelling light reflected at the sea surface back into the atmosphere was not included in L_w. For the spectral modeling, we used the following wavelengths (mostly centers of SeaWiFS and MODIS bands): 300, 412, 443, 493, 510, 531, 551, 600, 667, 678, 748, 765 and 800 nm. Recent modeling results [5] show the importance of the depth weighting function for IOP averaging in applications involving approximate semi-analytical models based on explicit relationships between RSR and IOPs. This is especially important in the case of highly scattering water layers such as

bubble clouds. However, in this study the light field is calculated directly with a 3-D radiative transfer code, which does not require a depth weighting function for IOP averaging.
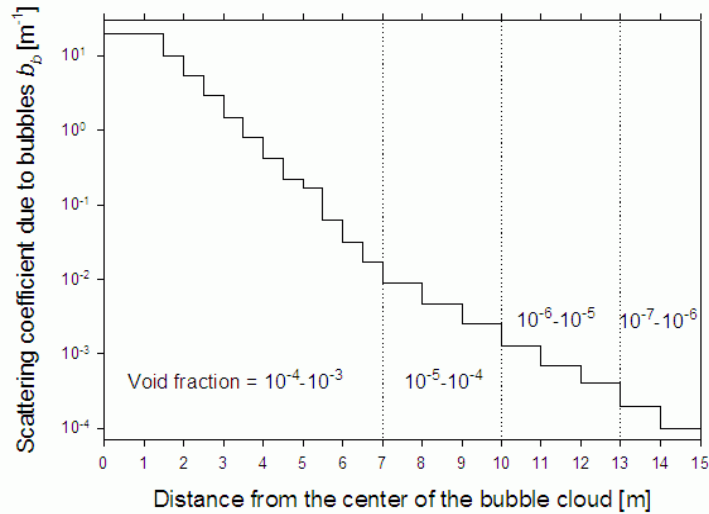

Fig. 1. Scattering coefficient of bubbles in the hemispherical model as a function of distance from the cloud center. The phase functions used corresponded to the assumed void fractions.
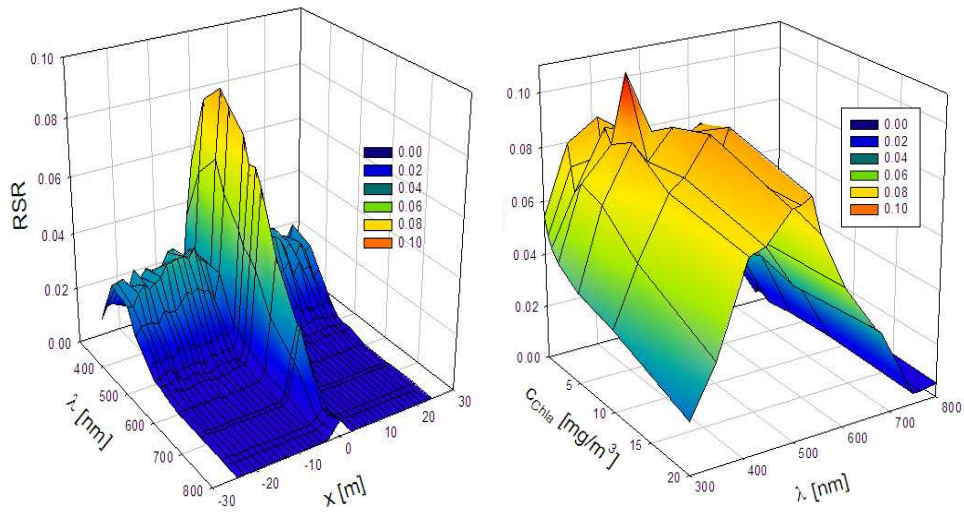

Fig. 2. Remote-sensing reflectance for a hemispherical model of the bubble cloud defined in Fig. 1. (a) RSR across a bubble cloud (x axis) as a function of light wavelength. Non-bubble IOPs correspond to chlorophyll concentration of 0 mg/m^3, meaning that the 'background' IOPs are defined by absorption and scattering by pure seawater; (b) RSR just above the center of the bubble cloud as a function of light wavelength and chlorophyll concentration.

3. Results and discussion

Figure 2a presents an example of the spectral dependence of the RSR across the hemispherical bubble cloud for sea water with chlorophyll *a* concentration Chla = 0 mg m^{-3}. As the IOPs of non-bubble seawater constituents (particulate and dissolved matter) in our model were parameterized as a function of Chla, this model scenario means that the background IOPs are

defined solely by pure seawater absorption and scattering. The strong enhancement of the RSR within the central portion of the bubble cloud (i.e., within a few meters of x = 0) is clearly seen. The drastic reduction of the RSR away from the cloud center is associated with significant decrease in bubble scattering. In this particular case the bubble scattering coefficient dropped by ~2 orders of magnitude at 5 m from the center. Note also that the RSR values in the near-infrared (near-IR) are significantly higher than zero above the center of the cloud. This indicates that in the presence of bubble clouds, the ocean is not "black" in this near-IR region, which is in contrast with an assumption often used in remote-sensing algorithms. This was found even though inelastic scattering was not taken into account. Some background statistical random noise (inherent to Monte Carlo methods) is also seen, especially for the blue wavelengths.

Figure 2b shows the RSR over the center of the hemispherical bubble cloud as a function of wavelength and chlorophyll concentration. We recall that the latter serves as a proxy for IOPs associated with non-bubble seawater constituents. The results show much less statistical noise than the "rough" shape of the RSR pattern might suggest. We expect almost no methodological bias as the random number generator used in the Monte Carlo code has a period of more than 2^{127} and well-tested uniformity. The statistical noise appears visible, especially in the blue spectral region for low chlorophyll concentrations (due to the linear scale of the graph). The interesting peak at $\lambda = 443$ nm and Chla = 2.0 mg m^{-3} seems real as the result was confirmed by recalculation with the same input data but a different seed of the random number generator. Therefore, Fig. 2b indicates that the RSR over the bubble cloud depends strongly, and evidently in a rather complex manner, on the mixing of optical properties associated with bubbles and other optically significant water constituents within the bubble cloud.
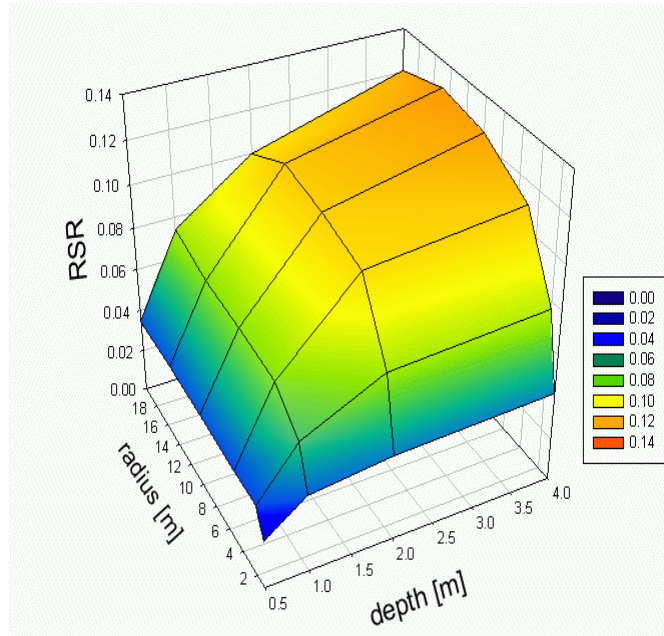

Fig. 3. Remote-sensing reflectance over the center of a uniform cylindrical dense (b_{bub} = 20 m^{-1}, Chla = 5 mg m^{-3}) bubble cloud as a function of the cloud radius and depth.

Figure 3 shows the results from simulations of uniform cylindrical bubble clouds with high scattering, b_{bub} = 20 m^{-1}. In this case we did not use multiple layers with decreasing scattering away from the center of the bubble cloud but we examined different horizontal (radius) and vertical (depth) extents of the cloud. With an increasing bubble radius, the RSR

measured above the center of the cloud initially increases and then reaches an approximate plateau for radii larger than about 10 m. This is observed regardless of the depth of the bubble cloud. The plateau means that the effects originating within the margins of the bubble cloud no longer influence appreciably the reflectance above the cloud center. Therefore, we may expect that a bubble cloud with a dense core having an overall horizontal extent (2 x radius) > 20 m is needed to achieve conditions in the cloud center comparable to what would be predicted for a layered bubble cloud from a 1-D radiative transfer model with plane-parallel geometry. The size of most bubble clouds, especially the size of the central region with high scattering, is expected to be generally significantly smaller than 20 m, so not surprisingly we can conclude that the 1-D approach is inadequate for modeling light fields within and leaving the bubble clouds.
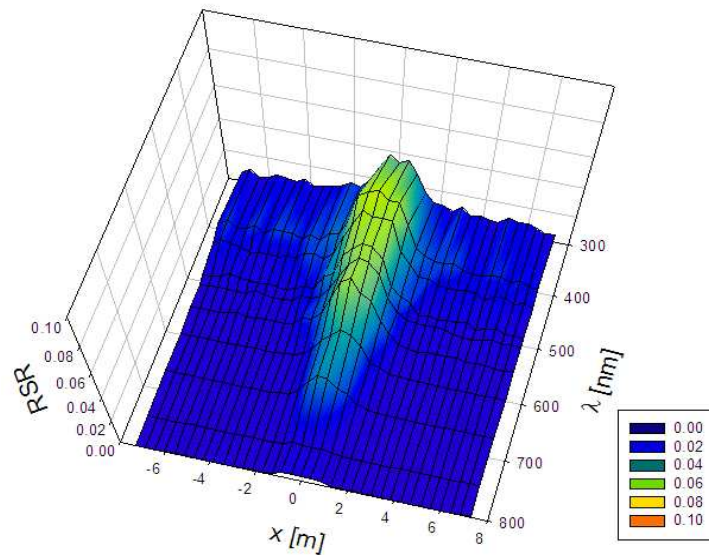

Fig. 4. Remote-sensing reflectance across the bubble cloud (x-axis) as a function of light wavelength for a cylindrical model of the cloud. The radius of the cloud is $r = 1$ m and depth $d = 2$ m with $b_{bub} = 20$ m^{-1}. The 'background' IOPs of seawater correspond to the chlorophyll concentration of 1 mg m^{-3}.

Example effects revealed with 3-D modeling of cylindrical bubble clouds are shown in Figs. 4 and 5. One of the 3-D effects is the spectrally-dependent footprint of enhanced reflectance produced by the bubble cloud (Fig. 4). The horizontal extent of this signature appears to narrow towards the red and near-IR portion of the spectrum as the absorption coefficient of water increases. At wavelengths with lower absorption the size of the reflectance footprint is larger because photons scattered within the bubble cloud are able to travel father away from the central portions of the cloud before propagating through the sea surface into the atmosphere. As a result, for measurements of reflectance with high spatial resolution, the spectrally variable size of the bubble cloud footprint may influence the spatially-averaged reflectance to varying extents at different wavelengths. These influences are obviously expected to increase with decreasing pixel size over which the spatial averaging of reflectance is made.

Another interesting feature seen in the 3-D results, especially at wavelengths with high water absorption such as 800 nm, is a secondary maximum of the RSR that develops close to the edges of sharply defined bubble cloud. This "rim" effect is caused by photons that enter a bubble cloud from surrounding water and are subsequently scattered upwards towards the water surface. The high absorption of seawater is necessary to observe this feature because it makes the average photon pathlength short enough to prevent side radiation from penetrating

the bubble cloud deeper towards its center. Also, Fig. 5 shows that the size of the bubble cloud has to exceed a certain threshold for the rim effect to develop.
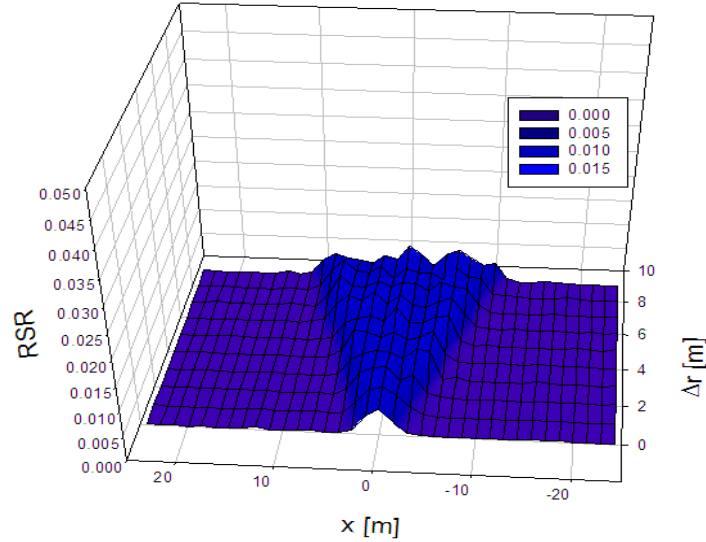

Fig. 5. Remote-sensing reflectance across the bubble cloud (x-axis) as a function of the radius of the cloud. These results were obtained for a cylindrical model of the bubble cloud similar to that of Fig. 3 but with variable radius $r = 1$ m $+ \Delta r$ and for the light wavelength of 800 nm and the chlorophyll concentration of 1 mg m^{-3}.

4. Conclusions

The 3-D modeling results show that high-spatial resolution patterns of ocean reflectance are quite complex over a bubble cloud and depend on geometry and optical properties of bubble clouds, including the optical contributions of non-bubble water constituents (water molecules, suspended particles, and organic dissolved matter). These patterns are also dependent on the light wavelength. The RSR produced by bubble clouds is generally not negligible in the near-IR, which has ramifications for the methodology of atmospheric correction in remote sensing algorithms. Our 3-D simulations of radiative transfer also provide evidence that 1-D modeling with plane-parallel geometry will be generally inadequate for modeling light fields within and leaving the bubble cloud. Our results show several 3-D effects. For example, there is a reduced size of the bubble reflectance footprint in the spectral region with high seawater absorption, most specifically in the red/near-infrared portion of the spectrum where molecular water absorption is high, and the "rim" effect that manifests itself as the development of the secondary maximum in the reflectance above the margins of dense bubble clouds (in addition to the primary maximum observed above the center of the cloud), especially under conditions of high absorption by seawater. The complexity of the optical effects of bubble clouds and their potential significance for remote sensing justify further research.

Acknowledgments